

# <sup>3</sup>He refrigerator based very low temperature scanning tunneling microscope

S. H. Pan, E. W. Hudson, and J. C. Davis

*Department of Physics, University of California, Berkeley, California 94720*

(Received 3 September 1998; accepted for publication 27 October 1998)

We describe the design and development of a scanning tunneling microscope (STM) which can operate at temperatures down to 240 mK and in magnetic fields up to 7 T with high spatial and energy resolution. The compact and rigid STM head is mounted directly on a low vibration, single shot, <sup>3</sup>He refrigerator. This refrigerator can be operated at its base temperature continuously for several days before the <sup>3</sup>He needs to be recondensed. The system is equipped with a sample transport manipulator from room temperature, and a cleavage device at low temperature, so that the cryogenic ultrahigh vacuum condition inside the cryostat can be utilized. A superconducting magnet provides a magnetic field of up to 7 T at the sample along the STM tip direction. Test results have shown that, at the base temperature, this instrument has better than 0.5 pm *z*-direction resolution in imaging mode, and better than 20  $\mu$ V energy resolution in spectroscopy mode. © 1999 American Institute of Physics. [S0034-6748(99)00802-3]

## I. INTRODUCTION

An important direction for the development of scanning tunneling microscopes (STMs) is towards applications in the millikelvin temperature range. Such instruments will allow the study of physical phenomena that do not occur until very low temperatures are reached, for example, superconducting phase transitions in heavy fermion materials. Even with phenomena that occur and are observable at higher temperatures, energy resolution (which is limited by thermal broadening) can be dramatically improved if the measurements are performed at millikelvin temperatures. Although numerous STM instruments have produced results near 4.2 K, few have been used at much lower temperatures.<sup>1,2</sup> In this article, we report on the development of a very low temperature STM for operation in a magnetic field with very high spatial and spectroscopic resolution.

## II. INSTRUMENT DESIGN

To design an STM which can achieve atomic resolution while operating at very low temperatures is a challenging task. Operation at low temperatures brings the benefits of low thermal drift and low thermal noise, which are required for high-resolution measurements. On the other hand, very low temperature refrigeration techniques often hamper the efforts to achieve high-resolution measurements due to the introduction of mechanical vibrations. Furthermore, the physical space within the cryostat, especially when a high magnetic field is required, is often too limited to allow an effective cryogenic vibration-isolation stage. Our efforts to address these challenges are concentrated in the following three elements: (1) a very rigid STM head that is less susceptible to vibration, (2) a refrigeration scheme that has very low intrinsic vibrational noise, and (3) a good external vibration-isolation system to reduce transmission of vibrations from the external environment to the STM cryostat.

### A. STM head

To fit into the limited space inside the refrigerator and to adapt to the configuration of the refrigeration scheme, our STM head is required to be compact and arranged for top loading of samples. Figure 1 shows a schematic diagram of the STM head. It integrates a tube scanner and coarse-approach motor into a main body (8) machined from a single piece of Macor (a machinable ceramic produced by Corning Incorporated).<sup>3</sup> On top of the body is a spring loaded sample receptacle (1) machined from brass, which makes strong electrical and thermal contact to the sample holder (2), and thus to the sample, when it is loaded from above. The coarse-approach mechanism is a piezo actuated motor that consists of the main body (8), a spring press-plate (9), six shear-piezo stacks with ceramic contact pads glued on top (7), and a prism-shaped sapphire shaft (6) with a hole in the center.

Such a motor has been described in detail elsewhere.<sup>4</sup> The schematic drawing in Fig. 2 briefly illustrates its working principle. Four piezo legs hold a moving shaft in position. When a voltage is applied to one leg, it slides backward (to the right) along the surface of the shaft, as friction between the other three legs and the shaft holds the shaft stationary. After an appropriate delay, the same voltage as was applied to the first leg is applied to one of the other piezo legs. Once again, the shaft keeps its original position without movement while this second leg slides backward along the sapphire surface. Finally, after all legs have been independently slid backwards one after the other, the voltages on all legs are ramped down simultaneously, as shown in the drawing. Consequently, all the legs together carry the shaft one step forward (to the left). This design has been proven to have some unique features which are suitable for use in very low temperature scanning probe instruments.<sup>5,6</sup> Most important of all, the motor is very reliable, with reproducible step sizes. In addition, since it does not rely on inertia, it can be operated in a vertical direction with minimal step-size differ-

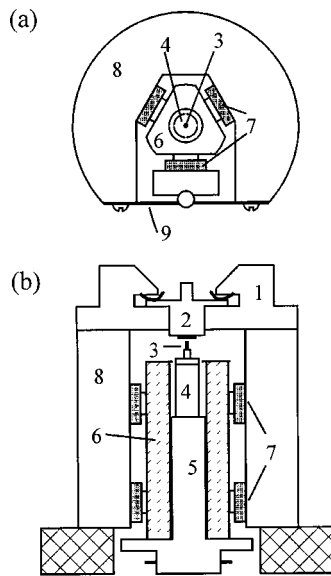


FIG. 1. STM head, (a) top view (with sample receptacle removed for clarity) and (b) side view. 1.5 in. in diameter by 1.75 in. high. (1) Sample receptacle, (2) sample holder, (3) tip, (4) tube scanner, (5) scanner holder, (6) sapphire prism, (7) shear piezo stacks, (8) macor body, (9) spring plate (*not to scale*).

ences due to gravity. This is an important feature as it allows a compact design suitable for use in the most common top loading refrigerators and in small bore, high field, solenoid magnets. Furthermore, the piezo legs constantly clamp the moving shaft and no voltage is required to keep the shaft in position while it is stationary. Thus the entire structure is rigid and stable. The piezo motor in our STM head has a step size of about 2000 Å at room temperature and about 300 Å at temperatures below 4 K, when driven with a peak voltage of 300 V. One can easily vary the step size by changing the applied voltage.

As shown in Fig. 1, a 1/8 in. diameter piezotube scanner (4) is glued with epoxy onto the scanner holder (5), which is also machined from Macor. This assembly is then mounted into the hole in the sapphire prism (6). The assembly of (4) and (5) can easily be changed to obtain various scan ranges.

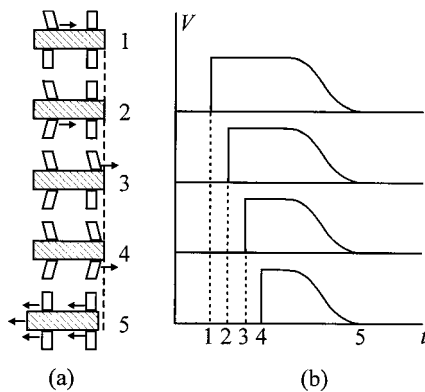


FIG. 2. Schematic illustration of the working principle of the piezo coarse approach motor. (a) The sequence of motions of shear piezo stacks and the sapphire prism. (b) The sequence of voltages applied to each piezo leg to produce the motions in (a).

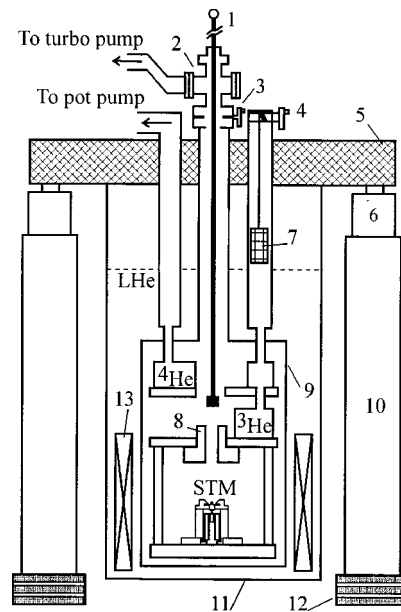


FIG. 3. STM cryostat and vibration-isolation table. (1) Manipulator rod, (2) load-lock chamber, (3) gate valve, (4) charcoal sorption pump lift/lowering mechanism, (5) table top of the vibration-isolation table, (6) air-spring, (7) activated charcoal sorption pump, (8) mechanical sample cleavage stage, (9) vacuum chamber, (10) supporting leg, (11) superinsulation Dewar, (12) stacked rubber and steel pads, (13) 7 T magnet (*not to scale*).

The tip holder in our design is a fine metal tube glued into a ceramic tube and then glued on top of the tube scanner. The tip (3) is held in the fine tube simply by friction.

The design of the STM head is simple and compact. It has a dimensions of 1.75 in. in height and 1.5 in. in diameter.

## B. Refrigeration, thermometry, and superconducting magnet

The refrigeration scheme used in this setup is a specially designed, low noise, single shot,  $^3\text{He}$  sorption refrigerator. As shown in the schematic drawing of Fig. 3, the refrigerator is housed in a vacuum can (9) which is immersed in a liquid helium bath inside a superinsulated Dewar.<sup>7</sup> The small (4.5 in. diameter) but long (3 ft.) neck of the Dewar reduces the boil-off rate of the liquid helium to about 4 ℓ/day (with the superconducting magnet installed) and thus also reduces vibrations due to evaporation of the liquid  $^4\text{He}$  in the bath. A 750 ℓ/min rotary pump is used to pump on the  $^4\text{He}$  pot, which is inside the vacuum can, to achieve a temperature of 1.2 K at the  $^4\text{He}$  stage. This temperature will condense the  $^3\text{He}$  sample into about 10 cc of liquid in the  $^3\text{He}$  pot. An activated charcoal pump (7), when lowered into the 4.2 K region by a lift mechanism (4), pumps on the condensed  $^3\text{He}$  to achieve a base temperature of 220 mK at the  $^3\text{He}$  stage. To achieve this temperature, all mechanical and electrical connections from room temperature must be minimized and carefully heat sunk. Radiation from room temperature is also carefully baffled. With these measures, 10 cc condensed  $^3\text{He}$  can keep the refrigerator at 220 mK for about three days before recondensation is needed.

At the STM head we reach a base temperature of 237 mK. A commercially calibrated Cernox thermometer<sup>8</sup> is attached to the sample receptacle to ensure accurate measure-

ment of the sample temperature. Since the sample surface faces inwards, we believe that it reaches the equilibrium temperature of the sample receptacle as measured by the calibrated Cernox thermometer. We have verified that the STM tip also cools to this temperature by fitting tunneling spectra from a superconducting Nb tip to BCS theory.<sup>9</sup> All thermometers are carefully thermally anchored to the measuring points and operated with low current, low frequency ac bridge circuits, thus avoiding self-heating. We also fastened a resistive heater on the base plate of the STM to vary the base temperature when needed. The operation of the refrigerator is rather simple and straightforward. One can cool the STM from room temperature down to the base temperature of 240 mK in less than 36 h.

A 7 T superconducting solenoid with 4.5 in. bore<sup>10</sup> is installed in the bottom of the <sup>4</sup>He Dewar and surrounds the stainless steel vacuum can of the refrigerator. The sample receptacle on the STM head is located at the center of the homogeneous (0.1% over 1 cm DSV) region of the magnetic field. The two current leads of the superconducting magnet are detachable. When the magnetic field is stabilized at the desired field strength and set in persistent mode, the current leads are detached from the magnet and brought out of the liquid bath to reduce the <sup>4</sup>He boil-off. With such an arrangement, the entire system has a <sup>4</sup>He boil-off rate of about 5 ℓ per day. Hence, the 16 ℓ capacity of the Dewar gives about three days of operation, matching the length of the continuous operation time of the <sup>3</sup>He fridge for a single dose. All materials used in the refrigerator and STM head are nonmagnetic. We have successfully operated the STM at the maximum field of 7 T.

### C. Vacuum System

A 60 ℓ/s turbopump pumps the 4 ℓ stainless steel vacuum can (4 in. in diameter by 21 in. long) via the load-lock chamber (2) (a four-way cross), the gate valve (3), and a 5/8 in. diameter, 40 in. long, stainless steel tube. The vacuum has been measured at the load-lock chamber as  $4 \times 10^{-6}$  Torr at room temperature after 12 hours of pumping without baking. A 6 ft long manipulator rod (1) that passes through a home-built, differentially pumped feedthrough allows us to transfer samples from room temperature down to the STM which remains at low temperatures. Such an arrangement not only greatly reduces experimental turn around time, but also enables us to utilize the ultrahigh vacuum (UHV) conditions at very low temperatures for *in situ* tip cleaning by field-emission and sample cleavage. A mechanical sample cleavage stage (8) is directly mounted on the <sup>3</sup>He refrigerator for cleaving samples at low temperatures.

### D. Vibration Isolation

Early tests showed that our STM head is very rigid and our charcoal pump based refrigerator is vibrationally quiet. Hence, we did not need to use the originally designed low temperature vibration-isolation stage.<sup>11</sup> Instead, we have bolted the STM to a solid frame, made of OFHC copper and plated with gold, that directly extends from the coldest stage of the fridge. This frame supports the STM head vertically,

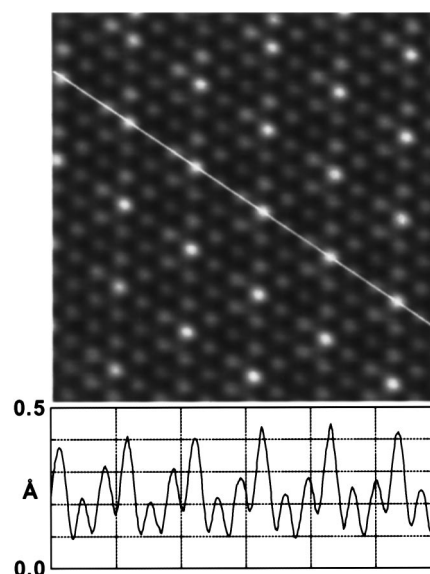


FIG. 4. Constant current image on NbSe<sub>2</sub> at 240 mK. ( $I = 50$  pA,  $V_{\text{sample}} = -50$  mV,  $50 \text{ \AA}$  scan range) below the image a line-profile position marked on the image shows the apparent atomic corrugation and CDW modulation.

with sample receptacle facing upward for top loading of samples. Eliminating the vibration isolation between the STM and the refrigerator greatly simplifies the arrangement of thermal and electrical connections.

Thus, all vibration isolation is external and at room temperature. As depicted in Fig. 3, the refrigerator is mounted below a home built vibration-isolation table. The triangular shaped tabletop (5) is filled with lead shot (weighing about 1000 pounds) and sits on top of three commercial air springs. Three legs filled with concrete support the air springs to elevate the refrigerator to a height where one can comfortably work on the STM. Beneath these legs, rubber and steel pads are stacked to serve as a first vibration damper. The entire system is housed in a home-built acoustic-isolation room and all control electronics are placed in an adjacent room to avoid the vibrational noise from cooling fans and movement of the operators. All mechanical pumps are located in a separate basement, except for the turbopump. During STM operation, the gate valve above the vacuum chamber is closed and the turbopump is turned off. Cryogenic temperatures guarantee maintenance of good vacuum in the vacuum chamber.

## III. EXPERIMENTAL RESULTS

Our initial tests of the STM at both room temperature and low temperatures were performed on highly oriented pyrolytic graphite (HOPG). Further tests were then performed on 2H-NbSe<sub>2</sub>, a well-studied material that has both charge density wave (CDW) and superconducting phase transitions at low temperatures, and thus is ideal for test and calibration. As it is a type II superconductor, a moderate magnetic field (0–3 T) produces a vortex lattice which can be imaged to test operation in a magnetic field.

In Fig. 4, we show a constant current image on NbSe<sub>2</sub> at a temperature of 250 mK. Both the atomic corrugation and

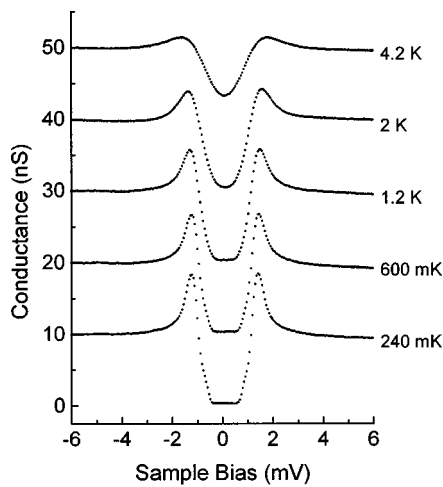


FIG. 5. Set of  $dI/dV$  curves measured with lock-in amplifier on the same sample as in Fig. 4 at various temperatures. (Modulation frequency  $f_{\text{mod}} = 331$  Hz, amplitude  $A_{\text{mod}}$  is  $40 \mu\text{V}_{\text{rms}}$  for the curve at 240 mK and  $80 \mu\text{V}_{\text{rms}}$  for the rest, 288 data points in 20 min acquisition time for each curve.) The curves are offset for clear display. The temperature dependence of the superconducting energy gap is well resolved.

the CDW modulation are clearly resolved. Below the image, a line profile, position marked with a white line on the image, shows that the noise level is in the order of 0.5 pm. This is consistent with the noise on our high voltage amplifiers for the scan piezo. Note that all data shown in this article is original and unfiltered (the only image processing employed is plane subtraction leveling).

To demonstrate high-resolution spectroscopy on the same sample, we show in Fig. 5 a set of  $dI/dV$  curves measured by a lock-in technique at various temperatures. The curves are offset in 10 nS steps for clear display. The temperature dependence of the superconducting energy gap is clearly resolved. The modulation amplitude used was  $40 \mu\text{V}_{\text{rms}}$  for the curve at 240 mK and  $80 \mu\text{V}_{\text{rms}}$  for the rest. We have also successfully used a  $10 \mu\text{V}_{\text{rms}}$  modulation amplitude for the same measurement at 240 mK.

Figure 6 displays Abrikosov flux lattice and vortex core images taken on  $\text{NbSe}_2$  to demonstrate stable operation in a magnetic field. We image the vortices by setting the junction resistance at a given bias ( $100 \text{ M}\Omega$  at 10 mV in these cases)

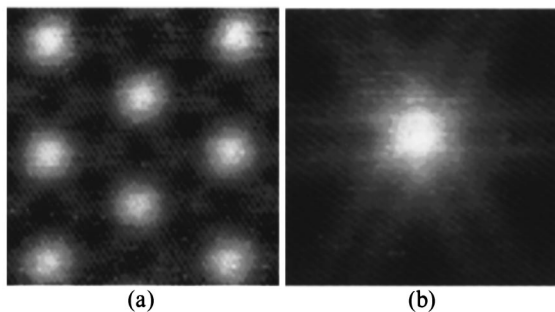


FIG. 6. Differential conductance images (140 nm square) showing vortices on the surface of  $2\text{H-NbSe}_2$ . (a) A magnetic field of  $B = 0.90$  T was used, and the measurement was taken at a sample bias of  $V_{\text{sample}} = 0.0$  mV. (b)  $B = 0.25$  T,  $V_{\text{sample}} = -0.24$  mV. In both cases, the junction resistance was set to  $100 \text{ M}\Omega$  at  $V_{\text{sample}} = -10$  mV, and lock-in amplifier settings of  $f_{\text{mod}} = 447.3$  Hz and  $A_{\text{mod}} = 100 \mu\text{V}$  were used.

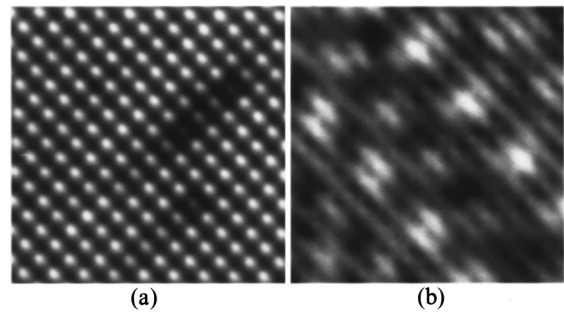


FIG. 7. Images of two surfaces which were exposed after cleavage of single crystal YBCO. (a) BaO plane ( $I = 1$  nA,  $V_{\text{sample}} = 100$  mV) with clear atomic resolution and several defects (darker sites). (b) CuO chain plane ( $I = 30$  pA,  $V_{\text{sample}} = 60$  mV), showing atomic resolution overlaid with a strong DOS modulation. Both images are  $50 \text{ \AA}$  square.

and then measuring the differential conductance at a low bias using a lock-in technique. The vortex lattice image in Fig. 6(a) was taken at 300 mK in a 0.9 T field. The vortex core displayed in Fig. 6(b) was imaged at 300 mK in a 250 mT field.

To demonstrate the concordant operation of the system, we also performed measurements on the high  $T_c$  superconductors  $\text{Bi}_2\text{Sr}_2\text{Cu}_2\text{O}_{8+x}$ <sup>12</sup> and  $\text{YBa}_2\text{Cu}_3\text{O}_{7-x}$  (YBCO). Both of these materials have complex crystal and electronic structures and sensitive surfaces, and hence care must be taken in order to obtain high-resolution results. Before inserting a sample, an electrochemically etched Pt/Ir tip is cleaned *in situ* by field emission against a single crystal gold target. The sample is then introduced through the load-lock chamber, cooled, and cleaved at low temperatures (below 20 K). This is particularly important for YBCO, as it prevents the surface deoxygenation which has been shown to occur when cleaved at higher temperatures.<sup>13,14</sup> Immediately after cleavage, the sample is transferred into the STM head, which is also at low temperature. These processes ensure the quality of the STM tip and sample surface for high-resolution imaging and spectroscopy measurements.

Figure 7 displays images of the two complementary surfaces which are exposed after cleaving YBCO single crystals.<sup>13</sup> The BaO plane [Fig. 7(a)] clearly shows a tetragonal lattice ( $\mathbf{a} \approx \mathbf{b} \approx 3.88 \text{ \AA}$ ), as well as several defects (that appear as 15 pm depressions on top of the background 12 pm corrugation height), which we believe to be due to oxygen deficiencies. The CuO chain plane image [Fig. 7(b)] shows a more complicated electronic structure. On top of a weak atomic corrugation (5 pm) is a much stronger density of states (DOS) modulation (30 pm) whose nature is the subject of current interest.<sup>15-17</sup>

#### IV. DISCUSSION

We have constructed a  $^3\text{He}$  refrigerator based very low temperature STM, which can reliably operate at temperatures down to 250 mK and in magnetic fields of up to 7 T. The test results of topographic and spectroscopic data demonstrate the capability of this system to perform both high spatial and spectroscopic resolution measurements at very low temperatures.

## ACKNOWLEDGMENTS

The authors would like to gratefully acknowledge A. Zettl for providing the 2H-NbSe<sub>2</sub> crystals and A. L. de Lozanne and J. T. Markert for the YBCO crystals. The authors thank R. Packard and A.L. de Lozanne for helpful conversations. They would also like to thank Topometrix Corporation for customizing their product and helping in further development, and American Magnetics and Kadel Engineering for working together to construct a low vibration, low boil-off Dewar with a high field magnet. This work was supported in part by the National Science Foundation under Grant No. 9458015, and by the Packard Foundation.

<sup>1</sup>H. F. Hess, R. B. Robinson, and J. V. Waszczak, *Physica B* **169**, 422 (1991).

<sup>2</sup>H. Fukuyama, H. Tan, T. Handa, T. Kumakura, and M. Morishita, *Czech. J. Phys.* **46**, 2847 (1996).

<sup>3</sup>Corning, Corning, NY.

<sup>4</sup>S. H. Pan, International Patent Publication Number WO 93/19494 (International Bureau, World Intellectual Property Organization), 30 September 1993.

<sup>5</sup>S. H. Pan, S. Behler, M. Bernasconi, H. Hidber, and H.-J. Güntherodt (unpublished).

<sup>6</sup>S. Behler, Ph.D. thesis, Inst. für Physik, Uni. Basel, Switzerland, 1993.

<sup>7</sup>Kadel Engineering, Danville, IN.

<sup>8</sup>Lake Shore Cryotronics, Inc., Westerville, OH.

<sup>9</sup>S. H. Pan, E. W. Hudson, and J. C. Davis, *Appl. Phys. Lett.* **73**, 2992 (1998).

<sup>10</sup>American Magnetics, Oak Ridge, TN.

<sup>11</sup>E. W. Hudson, R. W. Simmonds, C. A. YiLeon, S. H. Pan, and J. C. Davis, *Czech. J. Phys.* **46**, 2737 (1996).

<sup>12</sup>S. H. Pan, E. W. Hudson, J. Ma, and J. C. Davis, *Appl. Phys. Lett.* **73**, 58 (1998).

<sup>13</sup>H. L. Edwards, J. T. Markert, and A. L. de Lozanne, *Phys. Rev. Lett.* **69**, 2967 (1992).

<sup>14</sup>J. C. Campuzano, G. Jennings, M. Faiz, L. Beaulaigue, B. W. Veal, J. Z. Liu, A. P. Paulikas, K. Vandervoort, H. Claus, R. S. List, A. J. Arko, and R. J. Bartlett, *Phys. Rev. Lett.* **64**, 2308 (1990).

<sup>15</sup>A. L. de Lozanne, H. L. Edwards, C. Yuan, and J. T. Markert, *Acta Phys. Pol. A* **93**, 333 (1998).

<sup>16</sup>H. A. Mook, P. Dai, K. Salama, D. Lee, F. Dögan, G. Aeppli, A. T. Boothroyd, and M. E. Mostoller, *Phys. Rev. Lett.* **77**, 370 (1996).

<sup>17</sup>B. Grévin, Y. Berthier, G. Collin, and P. Mendels, *Phys. Rev. Lett.* **80**, 2405 (1998).